Temperature-dependent photoluminescence characterization of $Cd_{1-x-y}Be_xZn_ySe$ mixed crystals

2007 J. Phys.: Condens. Matter 19 096216

(http://iopscience.iop.org/0953-8984/19/9/096216)

IOP PUBLISHING JOURNAL OF PHYSICS: CONDENSED MATTER

J. Phys.: Condens. Matter **19** (2007) 096216 (11pp) doi:10.1088/0953-8984/19/9/096216

Temperature-dependent photoluminescence characterization of $Cd_{1-x-y}Be_xZn_ySe$ mixed crystals

J Z Wang[1], P J Huang[1], Y S Huang[1,4], F Firszt[2], S Łęgowski[2], H Męczyńska[2], A Marasek[2] and K K Tiong[3]

[1] Department of Electronic Engineering, National Taiwan University of Science and Technology, Taipei 106, Taiwan
[2] Institute of Physics, N Copernicus University, Grudziądzka 5/7, 87-100 Toruń, Poland
[3] Department of Electrical Engineering, National Taiwan Ocean University, Keelung 202, Taiwan

E-mail: ysh@mail.ntust.edu.tw

Received 5 December 2006, in final form 18 January 2007
Published 14 February 2007
Online at stacks.iop.org/JPhysCM/19/096216

Abstract

Temperature-dependent photoluminescence (PL) characterization of a series of wurtzite-type $Cd_{1-x-y}Be_xZn_ySe$ mixed crystals has been carried out in the temperature range between 15 and 300 K. The samples were grown by the modified high pressure Bridgman method. A typical PL spectrum at low temperature consists of an exciton line, an edge emission due to recombination of shallow donor–acceptor pairs and a broad band related to recombination through deep level defects. The peak positions of the excitonic emission line in the PL spectra correspond quite well to the transition energies of exciton A from previously reported electromodulation reflectance data (Liu *et al* 2005 *J. Appl. Phys.* **98** 083519). The parameters that describe the temperature dependence of the transition energy and broadening parameter of the band-edge excitonic emission are evaluated and discussed.

1. Introduction

Be-chalcogenide semiconductor alloys have recently been proposed for improving the performance of ZnSe-based blue–green lasers [1, 2]. It is expected that the incorporation of beryllium will lead to bond strengthening within the II–VI lattice, and will also increase the energy of stacking-fault formation, thus reducing defect propagation that has been seriously limiting the lifetimes of ZnSe-based devices. Among the Be-based II–VI compound semiconductors, $Cd_{1-x-y}Be_xZn_ySe$ solid solutions are of particular interest for their potential application in photodetectors operating in the visible and UV spectral region, in constructing green lasers and full-colour visible LEDs due to a large difference in the energy gaps E_g of

[4] Author to whom any correspondence should be addressed.

the constituents (CdSe, $E_g = 1.74$ eV; ZnSe, $E_g = 2.7$ eV; BeSe, $E_g = 5.5$ eV) [2, 3]. To date, in spite of their potential applications, very little work has been done on these quaternary compounds. There are some literature data concerning modulation reflectance and luminescence in zinc-blende (ZB) $Cd_{1-x-y}Be_xZn_ySe$ thin layers grown on InP [3, 4], but only a little is known about the basic optical and luminescence properties of $Cd_{1-x-y}Be_xZn_ySe$ bulk solid solutions [5, 6].

This report deals with a detailed temperature-dependent photoluminescence (PL) characterization of a series of wurtzite-type (WZ) $Cd_{1-x-y}Be_xZn_ySe$ mixed crystals with $0 < x \leqslant 0.15$ and $0 < y \leqslant 0.45$ in the temperature range of 15–300 K. The crystals were grown by the modified high pressure Bridgman method from the melt. PL spectra at low temperature consist of a sharp band-edge exciton line, a donor–acceptor pair (DAP) transition band and a broad deep level (DL) emission band. The nature of the DAP band has been discussed. The energy positions of the excitonic emission lines in the PL spectra are compared with previously reported electromodulation reflectance (ER) data [5]. The parameters that describe the temperature dependence of the transition energy and broadening parameter of the band-edge excitonic emission are evaluated and discussed.

2. Experimental details

$Cd_{1-x-y}Be_xZn_ySe$ mixed crystals were grown from the melt by the high-pressure Bridgman method [7] for $0 < x \leqslant 0.15$ and $0 < y \leqslant 0.45$. The CdSe (6 N Koch-Light), Be (purity >99%), Zn (purity 6 N) and Se (spectrographically standardized) powders were mixed in stoichiometric proportion and put into a graphite crucible. The crucible was kept for 10 h at 1873 K and then moved out from the heating zone at a speed of 2.4 mm h^{-1}. An argon overpressure of 13 MPa was maintained during the growth process. The obtained crystals were cut into plates of about 1 mm thickness, mechanically polished and chemically etched.

PL spectra were excited using the 325 nm line (∼40 mW) of a He–Cd laser. The luminescence signals were analysed by a SPEX 0.85 m double spectrometer and detected by a Hamamatsu photomultiplier tube. A closed-cycle cryogenic refrigerator equipped with a digital thermometer controller was used for temperature-dependent measurements. The luminescence spectra were recorded over a temperature range of 15–300 K with a temperature stability of 0.5 K or better.

3. Results and discussion

Figure 1 illustrates the PL spectra of four $Cd_{1-x-y}Be_xZn_ySe$ samples: $Cd_{0.94}Be_{0.03}Zn_{0.03}Se$ (sample I), $Cd_{0.8}Be_{0.1}Zn_{0.1}Se$ (sample II), $Cd_{0.6}Be_{0.1}Zn_{0.3}Se$ (sample III) and $Cd_{0.4}Be_{0.15}Zn_{0.45}Se$ (sample IV) at 15 K. At 15 K, the PL spectra consist of a narrow sharp peak (an exciton line denoted as X) followed by a broader emission band (DAP) at an energy 80–95 meV lower than the peak X and a broad deep level (DL) band. These low temperature PL spectra are generally similar to those of $Zn_{1-x}Be_xSe$ [8]. The sharp feature in the PL spectra shows a blue-shift in the transition energy and a line broadening with increase in the Be and Zn content. The line broadening for the samples with large Be/Zn content can be attributed in part to the alloy scattering effects and also to the poorer crystalline quality of the samples with higher content of incorporated Be. We have also observed a strong suppression of the DL emission at low temperature for sample I, an indication of a reasonably good quality crystal with a low Be ($x = 0.03$) content. In general, the intensity ratio of the peak X on the high energy side of the PL spectrum to that of the broad DL emission band can be used as an indicator of material

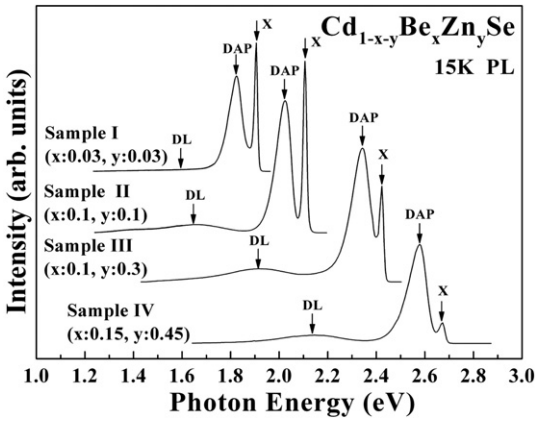

Figure 1. PL spectra of four $Cd_{1-x-y}Be_xZn_ySe$ samples: $Cd_{0.94}Be_{0.03}Zn_{0.03}Se$ (sample I), $Cd_{0.8}Be_{0.1}Zn_{0.1}Se$ (sample II), $Cd_{0.6}Be_{0.1}Zn_{0.3}Se$ (sample III) and $Cd_{0.4}Be_{0.15}Zn_{0.45}Se$ (sample IV) at 15 K.

quality. However, it is worth mentioning that the sharp peak X (exciton emission as will be discussed later) is observed in the temperature range from 15 K to room temperature in all investigated samples indicating that the quality of crystals is rather good.

The temperature evolution of the PL spectra for the four samples is plotted in figures 2(a)–(d), respectively. It can be seen that at the higher energy side the peak X shifts monotonically towards lower energy with increasing temperature in the range from 15 to 300 K and the broader band (DAP) is completely thermally quenched at temperatures higher than about 100 K. To examine the origin of these two near band-edge luminescence features, excitation intensity-dependent PL measurements were also been carried out at 15 K. Figure 3 illustrates the power density dependence of the luminescence intensity of the peak X and peak positions of these two features for sample II ($Cd_{0.8}Zn_{0.1}Be_{0.1}Se$). As shown in figure 3, the emission energy of peak X is independent of the excitation intensity but its intensity (as illustrated in the inset of figure 3) rises almost linearly with the increase in the excitation intensity. The results indicate that this luminescence line is dominated by excitonic radiative recombination. On the other hand, the broader emission band shifts toward higher photon energies with increasing intensity of exciting radiation. Taking into account the blue-shift with increasing excitation intensity as well as the thermal quenching, the broader feature is interpreted as due to recombination of shallow donor–acceptor pairs (DAP). This emission is known in II–VI binary compounds and is commonly called the 'edge emission'.

It is not possible from the presented luminescence data to establish the exact nature of the centres responsible for this PL band, but taking into account the detailed investigations of luminescence and optically detected magnetic resonance (ODMR) in binary II–VI compounds (ZnSe, ZnS, CdS), one can conclude that this band is due to radiative recombination of shallow donor–acceptor pairs, where the acceptor is Li or Na substituting a cation in the crystal lattice, but the donor is an isolated group III element in a cation site, Li interstitial or V_{Se}–Li_{Zn} complex. This kind of luminescence was always observed in all ZnSe/CdSe-based crystals grown in our laboratory with the same Bridgman method using the same ZnSe and CdSe powder as in this work. Figure 4 shows the temperature dependence of the integrated intensity of the DAP emission band for sample II. The value of the activation energy is determined to be 75 ± 5 meV from the thermal quenching observed for the DAP band. This value is considerably smaller than that of ZnSe and $Zn_{1-x}Mg_xSe$ reported by Firszt [9].

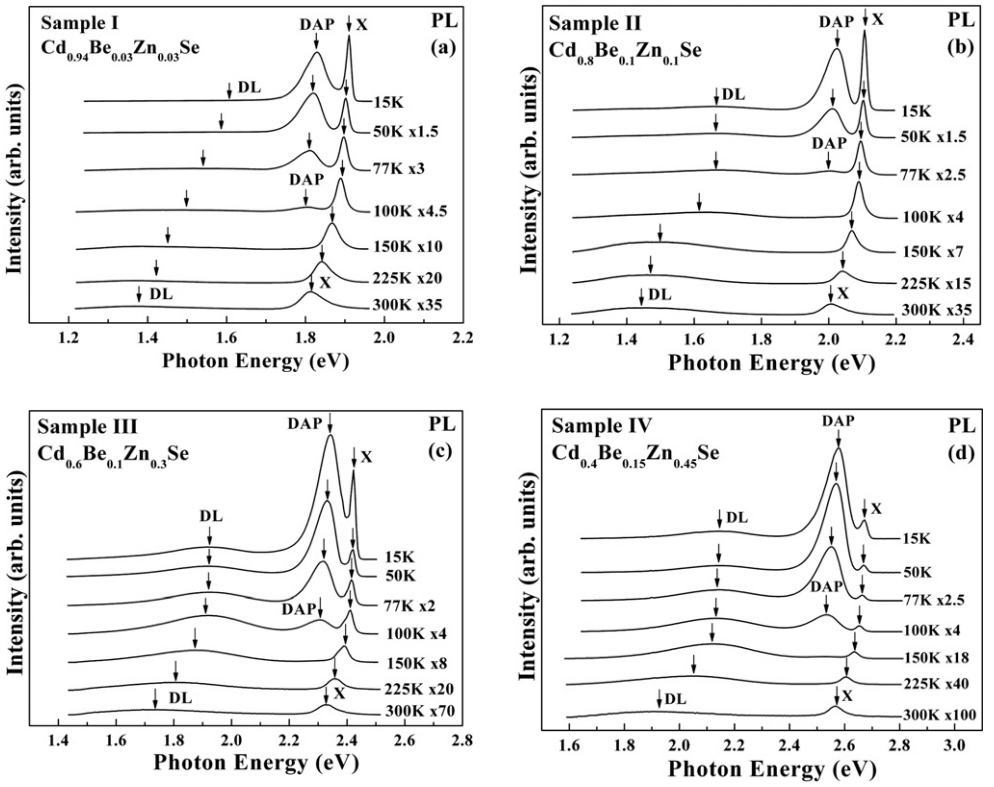

Figure 2. PL spectra of (a) $Cd_{0.94}Be_{0.03}Zn_{0.03}Se$ (sample I), (b) $Cd_{0.8}Be_{0.1}Zn_{0.1}Se$ (sample II), (c) $Cd_{0.6}Be_{0.1}Zn_{0.3}Se$ (sample III) and (d) $Cd_{0.4}Be_{0.15}Zn_{0.45}Se$ (sample IV) at several temperatures between 15 and 300 K.

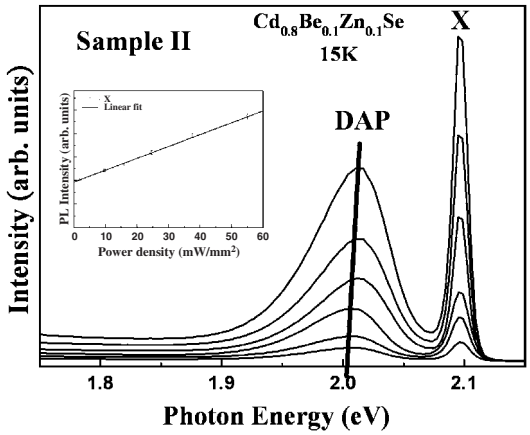

Figure 3. Power density-dependent peak positions for the two near band-edge luminescence features of $Cd_{0.8}Be_{0.1}Zn_{0.1}Se$ and power density-dependent luminescence intensity for peak X (inset).

We will henceforth focus on the temperature dependence of the band-edge exciton peaks. As shown in figure 2, like most semiconductors, when the temperature is increased,

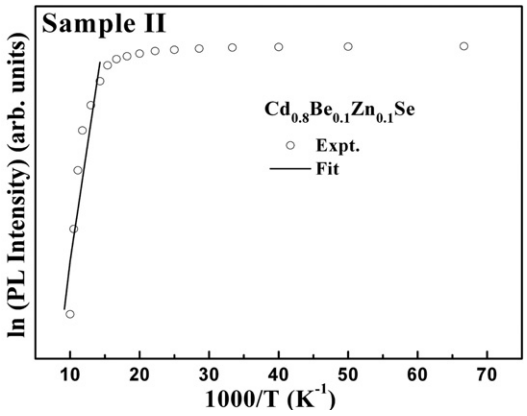

Figure 4. The thermal quenching of the intensity for the DAP emission band of $Cd_{0.8}Be_{0.1}Zn_{0.1}Se$.

the excitonic transitions in the PL spectra exhibit monotonically red-shifted and line-shape broadening characteristics. The line broadening of the features is mainly due to the increase of exciton–phonon interaction effects. Plotted by the open squares, open diamonds, open circles and open triangles in figure 5 are the temperature variations of the peak positions with representative error bars for $Cd_{1-x-y}Be_xZn_ySe$ samples I, II, III and IV, respectively. For comparison purposes, the experimental values of exciton A for samples I, II and III obtained from electromodulation [5] are also depicted in figure 5 by solid squares, solid diamonds and solid circles, respectively. The full curve in figure 5 is a least-squares fit to the Varshni semi-empirical relationship [10] as given by equation (1),

$$E(T) = E(0) - \frac{\alpha T^2}{(\beta + T)}. \tag{1}$$

Here $E(0)$ is the energy at 0 K and α and β are constants. The constant α is related to the electron (exciton)-average phonon interaction and β is closely related to the Debye temperature [10]. The values obtained for $E(0)$, α and β are listed in table 1. For comparison, the parameters for the near-band-edge transition energies of ZB-$Cd_{1-x-y}Be_xZn_ySe$ [4], WZ-$Cd_{1-x-y}Be_xZn_ySe$ [5], ZB-ZnSe [11], ZB-$Zn_{0.56}Cd_{0.44}Se$ [11], WZ-CdSe [12], GaAs [13], InP [14] and WZ-GaN [15] are also listed in table 1.

The temperature dependence of the peak positions of the band-edge exciton lines can also be described by a Bose–Einstein-type expression [16]:

$$E(T) = E(0) - 2a_B/[\exp(\Theta_B/T) - 1], \tag{2}$$

where $E(0)$ is the transition energy at $T = 0$ K, a_B represents the strength of the electron (exciton)-average phonon interaction and Θ_B corresponds to the average phonon temperature. Shown by the dotted line in figure 5 is a least-squares fit to equation (2). The obtained values for the various fitting parameters are also given in table 1. For comparison purposes, the parameters for the near-band-edge transition energies of ZB-$Cd_{1-x-y}Be_xZn_ySe$ [4], WZ-$Cd_{1-x-y}Be_xZn_ySe$ [5], ZnSe [11], ZB-$Zn_{0.56}Cd_{0.44}Se$ [11], GaAs [13], InP [14] and WZ-GaN [15] are also listed in table 1.

The parameter α of equation (1) can be related to a_B and Θ_B in equation (2) by taking the high-temperature limit of both expressions. This yields $\alpha = 2a_B/\Theta_B$. Comparison of the numbers presented in table 1 shows that this relation is indeed satisfied. From equation (2), it is straightforward to show that the high temperature limit of the slope of the $E(T)$ versus

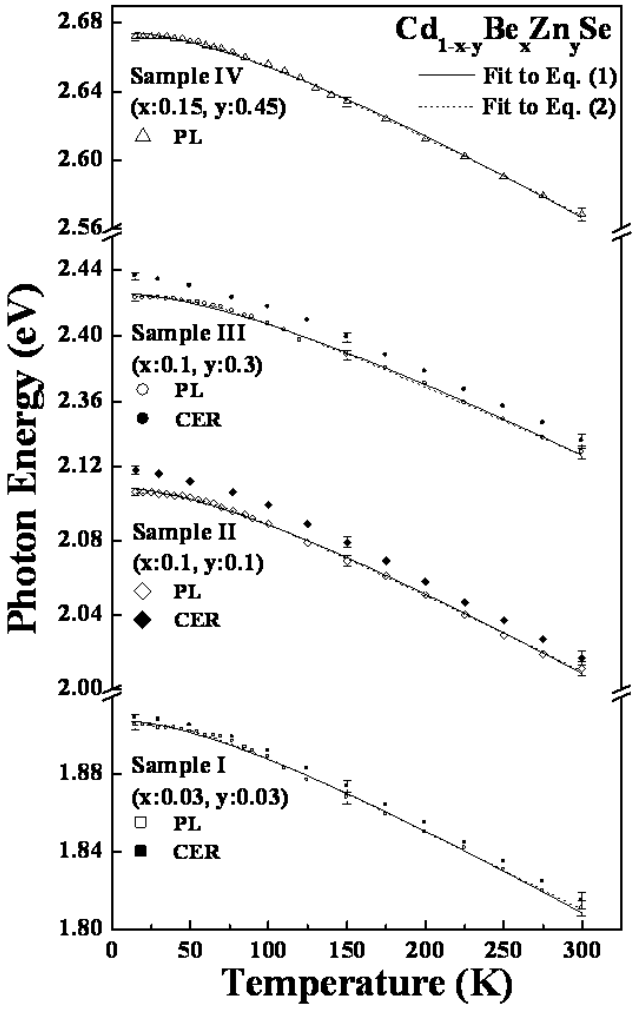

Figure 5. The temperature variations of the band-edge exciton peak positions with representative error bars for $Cd_{1-x-y}Be_xZn_ySe$ samples I, II, III and IV. The solid squares, diamonds and circles are the experimental values of exciton A for samples I, II and III, respectively, obtained from electromodulation [5]. The solid and dashed lines are least-squares fits to equations (1) and (2), respectively.

T curve approaches a value of $-2a_B/\Theta_B$. The calculated values of $-2a_B/\Theta_B$ for the band-edge exciton equal -0.415, -0.424, -0.431 and -0.475 meV K^{-1} for samples I, II, III and IV respectively, which agrees well with the values of $[dE_X/dT] = -0.398$, -0.40, -0.42 and -0.44 meV K^{-1} as obtained from the linear extrapolation of the high temperature (200–300 K) experimental data.

As depicted in figure 5, it should be noticed that for low Be and Zn content the peak positions of the band-edge exciton features in the PL spectra correspond quite well to the transition energies of the A exciton obtained from ER measurements [5]. A slightly different behaviour is observed for $Cd_{1-x-y}Be_xZn_ySe$ crystals with a high Be and Zn content.

In the case of photoexcitation, electron–hole pairs are generated at the entire absorption band range and then thermalized towards its bottom in a time much shorter than the radiative

Table 1. Values of the Varshni- and Bose–Einstein-type fitting parameters, which describe the temperature dependence of the energies of band-edge excitonic transitions of WZ-$Cd_{1-x-y}Be_xZn_ySe$ obtained from PL experiments. The parameters for WZ/ZB-$Cd_{1-x-y}Be_xZn_ySe$, ZB-ZnSe, WZ-CdSe, GaAs, InP and GaN are included for comparison.

Materials	Feature	$E(0)$ (eV)	α (10^{-4} eV K^{-1})	β (K)	a_B (meV)	Θ_B (K)
WZ-$Cd_{0.94}Be_{0.03}Zn_{0.03}Se$	X[a]	1.908 ± 0.003	4.8 ± 0.3	135 ± 30	32.9 ± 4	155 ± 20
	A exciton[b]	1.909 ± 0.002	4.53 ± 0.2	140 ± 20	28 ± 4	140 ± 30
WZ-$Cd_{0.8}Be_{0.1}Zn_{0.1}Se$	X[a]	2.108 ± 0.003	4.9 ± 0.3	144 ± 20	33.4 ± 3	157 ± 20
	A exciton[b]	2.117 ± 0.002	5.16 ± 0.2	140 ± 20	38 ± 5	170 ± 20
WZ-$Cd_{0.6}Be_{0.1}Zn_{0.3}Se$	X[a]	2.426 ± 0.003	5.1 ± 0.3	171 ± 20	35.8 ± 3	169 ± 20
	A exciton[b]	2.436 ± 0.002	5.20 ± 0.2	150 ± 40	40 ± 6	180 ± 20
WZ-$Cd_{0.4}Be_{0.15}Zn_{0.45}Se$	X[a]	2.675 ± 0.003	5.7 ± 0.3	175 ± 20	41.6 ± 3	175 ± 20
ZB-$Zn_{0.38}Cd_{0.62}Se$[c]	E_{hh}	2.138 ± 0.002	5.6 ± 0.2	195 ± 20	48 ± 4	195 ± 20
	E_{lh}	2.153 ± 0.002	5.7 ± 0.2	210 ± 20	50 ± 4	205 ± 20
ZB-$(Zn_{0.38}Cd_{0.62})_{0.93}Be_{0.07}Se$[c]	E_{hh}	2.203 ± 0.002	4.9 ± 0.2	180 ± 35	46 ± 4	205 ± 30
	E_{lh}	2.221 ± 0.002	5.1 ± 0.2	190 ± 35	45 ± 4	200 ± 30
ZB-$(Zn_{0.38}Cd_{0.62})_{0.89}Be_{0.11}Se$[c]	E_{hh}	2.242 ± 0.002	4.8 ± 0.2	175 ± 35	45 ± 4	205 ± 30
	E_{lh}	2.264 ± 0.002	4.8 ± 0.2	160 ± 35	44 ± 4	200 ± 30
ZB-ZnSe[d]	E_0	2.800 ± 0.005	7.3 ± 0.4	295 ± 35	73 ± 4	260 ± 10
ZB-$Zn_{0.56}Cd_{0.44}Se$[d]	E_0	2.272 ± 0.004	6.1 ± 0.5	206 ± 35	62 ± 4	236 ± 10
WZ-CdSe[e]	A exciton	1.834 (3)	4.24 (20)	118 (40)	36 (5)	179 (40)
GaAs[f]	E_0	1.512 ± 0.005	5.1 ± 0.5	190 ± 82	57 ± 29	240 ± 102
InP[g]	E_0	1.432 ± 0.007	4.1 ± 0.3	136 ± 60	51 ± 2	259 ± 10
GaN[h]	A exciton	3.490 ± 0.001	10.4 ± 0.8	1100 ± 100	75 ± 20	350 ± 50

[a] Present work (photoluminescence).
[b] Reference [5] (contactless electroreflectance/photoreflectance).
[c] Reference [4] (contactless electroreflectance).
[d] Reference [11] (contactless electroreflectance).
[e] Reference [12] (spectroscopic ellipsometry). The numbers in parentheses are error margins in unit of the last significant digit.
[f] Reference [13] (photoreflectance).
[g] Reference [14] (photoreflectance).
[h] Reference [15] (contactless electroreflectance).

life-time of excitons. It is known that the absorption and reflectivity spectra reflect the energetic distribution of the density of excitonic states, while the luminescence spectra are determined by their degree of filling. The common feature of ternary II–VI solid solutions is, as observed at low temperatures, a shift of the exciton luminescence line towards lower energies as compared to that of free exciton ground state determined from low temperature reflectivity spectra [17–19]. This feature is associated with an exciton localization process due to compositional disorder. In the investigated $Cd_{1-x-y}Be_xZn_ySe$ crystals with low Be and Zn (for example, sample I) content the energetic position of the maximum of the excitonic PL line is shifted a few meV towards lower energies from the corresponding energies of A excitons determined from the ER spectra in the temperature range from 15 K to room temperature (see figure 5). The character of the temperature dependence of the energetic position of the PL excitonic peak follows the ER data. For higher Be and Zn content, however, the difference between exciton energy determined from PL and ER spectra becomes noticeably larger at low temperatures (at around 15 K) than at higher ones. For the $Cd_{0.60}Be_{0.10}Zn_{0.30}Se$ sample, the difference between PL and ER data at 15 K is about two times larger than that at 300 K. This

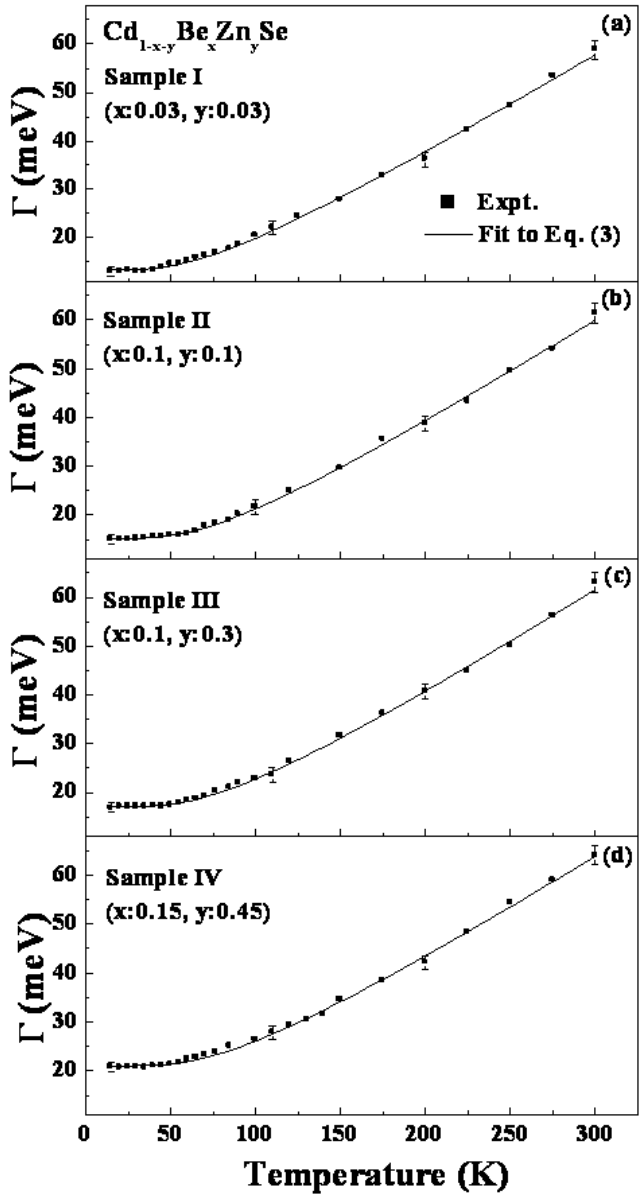

Figure 6. Temperature-dependent broadening parameters $\Gamma(T)$ for the band-edge exciton of (a) $Cd_{0.94}Be_{0.03}Zn_{0.03}Se$ (sample I), (b) $Cd_{0.8}Be_{0.1}Zn_{0.1}Se$ (sample II), (c) $Cd_{0.6}Be_{0.1}Zn_{0.3}Se$ (sample III) and (d) $Cd_{0.4}Be_{0.15}Zn_{0.45}Se$ (sample IV) with representative error bars. The solid lines are least-squares fits to equation (3).

is quite the opposite to the data for $Cd_{0.94}Be_{0.03}Zn_{0.03}Se$, where the PL and ER data are very similar. This indicates that some localization of excitons has taken place at low temperatures in $Cd_{1-x-y}Be_xZn_ySe$ crystals with a large Be and Zn content.

The experimental values of the temperature dependence of the line width $\Gamma(T)$ of the band-edge exciton emission are displayed in figures 6(a)–(d) for samples I–IV, respectively. Representative error bars are shown. Initially, $\Gamma(T)$ increases linearly with T, but begins to

Table 2. Values of the parameters that describe the temperature dependence of the broadening function Γ for edge excitonic transitions of WZ-$Cd_{1-x-y}Be_xZn_ySe$. The parameters for ZB-$Cd_{1-x-y}Be_xZn_ySe$, ZB-ZnSe, WZ-CdSe, GaAs, InP and GaN are included for comparison.

Materials	Feature	$\Gamma(0)$ (meV)	Γ_{LO} (meV)	Θ_{LO} (K)	γ_{ac} (μeV K^{-1})
WZ-$Cd_{0.94}Be_{0.03}Zn_{0.03}Se$	X[a]	13.4 ± 2	42.4 ± 8	211 ± 80	3 ± 1
	A exciton[b]	18 ± 2	38 ± 8	250 ± 80	3 ± 1
WZ-$Cd_{0.8}Be_{0.1}Zn_{0.1}Se$	X[a]	15.1 ± 2	47.8 ± 8	227 ± 90	3 ± 1
	A exciton[b]	19 ± 2	43 ± 8	270 ± 90	3 ± 1
WZ-$Cd_{0.6}Be_{0.1}Zn_{0.3}Se$	X[a]	17.7 ± 2	51.5 ± 8	242 ± 90	3 ± 1
	A exciton[b]	18 ± 2	50 ± 8	300 ± 90	3 ± 1
WZ-$Cd_{0.4}Be_{0.15}Zn_{0.45}Se$	X[a]	21.0 ± 2	54.4 ± 8	256 ± 90	3 ± 1
ZB-$Zn_{0.38}Cd_{0.62}Se$[c]	E_{hh}	3 ± 2	33 ± 8	320 ± 100	2 ± 1
	E_{lh}	4 ± 2	35 ± 8	310 ± 100	2 ± 1
ZB-$(Zn_{0.38}Cd_{0.62})_{0.93}Be_{0.07}Se$[c]	E_{hh}	17 ± 2	25 ± 8	330 ± 100	2 ± 1
	E_{lh}	18 ± 2	32 ± 8	335 ± 100	2 ± 1
ZB-$(Zn_{0.38}Cd_{0.62})_{0.89}Be_{0.11}Se$[c]	E_{hh}	19 ± 2	26 ± 8	345 ± 100	2 ± 1
	E_{lh}	20 ± 2	31 ± 8	350 ± 100	2 ± 1
ZB-ZnSe[d]	E_0	6.5 ± 2.5	24 ± 8	360[e]	2.0[e]
ZB-$Zn_{0.56}Cd_{0.44}Se$[d]	E_0	6.0 ± 2.0	17 ± 6	334[e]	1.1[e]
WZ-CdSe[f]	A exciton	2.3 (1)	23 (1)	300[e]	
GaAs[g]	E_0		23 ± 1.5	417[e]	
InP[h]	E_0	1.5 ± 0.5	31 ± 3.0	496[e]	
WZ-GaN[i]	A exciton	3.0 ± 0.5	250 ± 20	1065[e]	15[e]

[a] Present work (photoluminescence).
[b] Reference [5] (contactless electroreflectance/photoreflectance).
[c] Reference [4] (contactless electroreflectance).
[d] Reference [11] (contactless electroreflectance).
[e] A fixed parameter.
[f] Reference [12] (spectroscopic ellipsometry). The numbers in parentheses are error margins in unit of the last significant digit.
[g] Reference [13] (photoreflectance).
[h] Reference [14] (photoreflectance).
[i] Reference [15] (contactless electroreflectance), Ga face.

be superlinear starting from about 150 K. The temperature dependence of the line width of excitonic transitions of semiconductors can be expressed as [20]

$$\Gamma(T) = \Gamma(0) + \gamma_{AC}T + \frac{\Gamma_{LO}}{[\exp(\Theta_{LO}/T) - 1]}. \tag{3}$$

In equation (3), $\Gamma(0)$ represents the broadening invoked from temperature-independent mechanisms, such as electron–electron interaction, impurity, dislocation and alloy scattering, whereas the second term corresponds to lifetime broadening due to the exciton–acoustical phonon interaction with γ_{AC} being the acoustic phonon coupling constant. The third term is caused by the exciton–LO phonon (Fröhlich) interaction. The quantity Γ_{LO} represents the strength of the exciton–LO phonon coupling while Θ_{LO} is the LO phonon temperature [16, 20]. The full curves in figures 6(a)–(d) are least-squares fitted to equation (3) to evaluate $\Gamma(0)$, Γ_{LO}, Θ_{LO} and γ_{AC} for the band-edge exciton feature of samples I–IV, respectively. The obtained values of $\Gamma(0)$, Γ_{LO}, Θ_{LO} and γ_{AC} are listed in table 2. For comparison, the values of $\Gamma(0)$, Γ_{LO}, Θ_{LO} and γ_{AC} for ZB-$Cd_{1-x-y}Be_xZn_ySe$ [4], WZ-$Cd_{1-x-y}Be_xZn_ySe$ [5], ZnSe [11],

ZB-$Zn_{0.56}Cd_{0.44}Se$ [11], WZ-CdSe [12], GaAs [13], InP [14], and WZ-GaN [15] from other works are also included in table 2. The values of $\Gamma(0)$ for the Be-containing samples are much larger than those for Be-free samples, due mainly to the poorer crystalline quality of the Be-incorporated samples. In fact, it is not easy to grow high-quality Be-incorporated II–VI mixed quaternary samples. It is also noticed that the values of Γ_{LO} and Θ_{LO} become larger with increasing Be content. The larger values of Γ_{LO} and Θ_{LO} are presumably related to the higher effective longitudinal optical phonon energy of the Be-containing samples.

Our values for Γ_{LO} are comparable to those for ZB-$Cd_{1-x-y}Be_xZn_ySe$ [4], ZB-ZnSe [11], ZB-$Zn_{0.56}Cd_{0.44}Se$ [11], WZ-CdSe [12] and most of the III–V semiconductors [13, 14], with the exception of GaN [15]. It has been shown theoretically that the Fröhlich interaction is stronger for the higher ionicity II–VI semiconducting crystals, compared to that of the III–V semiconducting crystals [21]. Our results show no clear trend to that effect and seem to indicate that other factors may contribute to the electron (exciton)–LO phonon coupling constant, Γ_{LO}. In the case of GaN [15, 22], it may be possible that a larger deformation potential interaction may make a significant contribution to Γ_{LO} in addition to the Fröhlich interaction. The ionicity dependence of the Fröhlich interaction requires further consideration and more work needs to be done in this area. For instance, Raman measurements may be useful for addressing the ionicity dependence of the Fröhlich interaction.

4. Summary

A temperature-dependent photoluminescence study of four wurtzite-type $Cd_{1-x-y}Be_xZn_ySe$ mixed crystals has been carried out in the temperature range 15 K $\leqslant T \leqslant$ 300 K. At low temperatures PL spectra consist of an exciton line, a broader emission band due to recombination of donor–acceptor pairs and a broad band related to recombination through deep level defects. The sharp band-edge excitonic features in the PL spectra show a blue-shift in the transition energy and a broadened line width with increasing Be/Zn content. Comparison of PL and ER data for $Cd_{1-x-y}Be_xZn_ySe$ samples, shows that for a low Zn and Be content the peak positions of the excitonic emission lines in the PL spectra correspond quite well to the transition energies of the A exciton from the ER data. For samples with a high Be and Zn content, our study indicates that localization of excitons has taken place at the low measured temperatures. The temperature dependence of the band-edge exciton luminescence has been analysed by both Varshni- and Bose–Einstein-type expressions. The parameters extracted from both expressions by extending into the high temperature regime are found to agree reasonably well. The parameters that describe the temperature dependence of the broadening function of the band-edge exciton have also been studied. The values of $\Gamma(0)$ for the Be-containing samples are much larger than those of Be-free samples due mainly to the poorer crystalline quality of the Be-incorporated samples. The larger values of Γ_{LO} and Θ_{LO} are related to the higher effective LO phonon energy of the Be-containing samples.

Acknowledgments

JZW, PJH and YSH acknowledge the support of the National Science Council of Taiwan under project no. NSC 95-2221-E-011-171.

References

[1] Ivanov S V, Toropov A A, Shubina T V, Lebedev A V, Sorokin S V, Sitnikova A A, Kopev P S, Reuscher G, Keim M, Bensing F, Waag A, Landwehr G, Pozina G, Bergman J P and Monemar B 2000 *J. Cryst. Growth* **214/215** 109

[2] Ivanov S V, Nekrutkina O V, Sorokin S V, Kaygorodov V A, Shubina T V, Toropov A A, Kopev P S, Reuscher G, Wagner V, Geurts J, Waag A and Landwehr G 2001 *Appl. Phys. Lett.* **78** 404
[3] Maksimov O, Guo S P and Tamargo M C 2002 *Phys. Status Solidi* b **229** 1005
[4] Hsieh C H, Huang Y S, Ho C H, Tiong K K, Muñoz M, Maksimov O and Tamargo M C 2004 *Japan. J. Appl. Phys.* 1 **43** 459
[5] Liu Y T, Sitarek P, Huang Y S, Firszt F, Łęgowski S, Męczyńska H, Marasek A, Paszkowicz W and Tiong K K 2005 *J. Appl. Phys.* **98** 083519
[6] Wronkowska A A, Firszt F, Arwin H, Wronkowski A, Wakuła M, Strzałkowski K and Paszkowicz W 2006 *Phys. Status Solidi* c **3** 1193
[7] Paszkowicz W, Godwod K, Domagała J, Firszt F, Szatkowski J, Męczyńska H, Łęgowski S and Marczak M 1998 *Solid State Commun.* **107** 735
[8] Mintairov A M, Raymond S, Merz J L, Peiris F C, Lee S, Bindley U, Furdyna J K, Melehin V G and Sadchikov K 1999 *Semiconductors* **33** 1021
[9] Firszt F 1997 *Semicond. Sci. Technol.* **12** 272
[10] Varshni Y P 1967 *Physica (Utrecht)* **34** 149
[11] Malikova L, Krystek W, Pollak F H, Dai N, Cavus A and Tamargo M C 1996 *Phys. Rev.* B **54** 1819
[12] Logothetidis S, Cardona M, Lautenschlager P and Garriga M 1986 *Phys. Rev.* B **34** 2458
[13] Shen H, Pan S H, Hang Z, Leng J, Pollak F H, Woodall J M and Sacks R N 1988 *Appl. Phys. Lett.* **53** 1080
[14] Hang Z, Shen H and Pollak F H 1990 *Solid State Commun.* **73** 15
[15] Huang Y S, Pollak F H, Park S S, Lee K Y and Morkoç H 2003 *J. Appl. Phys.* **94** 899
[16] Lautenschlager P, Garriga M, Logothetidis S and Cardona M 1987 *Phys. Rev.* B **35** 9174
[17] Firszt F, Męczyńska H, Łęgowski S and Paszkowicz W 2004 *J. Alloys Compounds* **371** 107
[18] Mariette H, Triboulet R and Marfaing Y 1998 *J. Cryst. Growth* **86** 558
[19] Abdykadyrov A G, Baranovski S D, Berfin S Yu, Ivtchenko E D, Naumov A Yu and Reznitsky A N 1990 *J. Exp. Theor. Phys.* **98** 2056
[20] Lee J, Koteles E and Vassell M O 1986 *Phys. Rev.* B **33** 5512
[21] Rudin S, Reinecke T L and Segall B 1990 *Phys. Rev.* B **42** 11218
[22] Fischer A J, Shan W, Park G H, Song J J, Kim D S, Yee D S, Horning R and Goldenberg B 1997 *Phys. Rev.* B **56** 1077